Proceedings of the ASME 2009 International Design Engineering Technical Conferences &
Computers and Information in Engineering Conference
IDETC/CIE 2009
August 30 - September 2, 2009, San Diego, California, USA

DETC2009-87343

VIBRATION OF PLANETARY GEARS WITH ELASTICALLY DEFORMABLE RING GEARS PARAMETRICALLY EXCITED BY MESH STIFFNESS FLUCTUATIONS

Robert G. Parker
State Key Lab for Mechanical Systems and Vibration
Univ. of Michigan-SJTU Joint Institute
Shanghai Jiao Tong University
Shanghai, China
Email: parker.242@osu.edu

ABSTRACT

The parametric instability of planetary gears having elastic continuum ring gears is analytically investigated based on a hybrid continuous-discrete model. Mesh stiffness variations of the sun-planet and ring-planet meshes caused by the changing number of teeth in contact are the source of parametric instability. The natural frequencies of the time invariant system are either distinct or degenerate with multiplicity two, which indicates three types of combination instabilities: distinct-distinct, distinct-degenerate and degenerate-degenerate instabilities. By using the structured modal properties of planetary gears and the method of multiple scales, the instability boundaries are obtained as simple expressions in terms of mesh parameters. Instability existence rules for in-phase planet meshes are given. The instability boundaries are validated numerically.

INTRODUCTION

In order to maximize the power density and improve load sharing among the planets, planetary gears in numerous industries are designed to have thin rims, and this leads to elastic deflection of the gear bodies, especially the ring gear [1-3].

The vibration of planetary gears has been studied in [4-15]. These works model the ring gear as a rigid body. Wu and Parker [3] established an elastic-discrete model that includes planetary gear discrete degrees of freedom (rotational and translational) and ring gear elastic deflection. The modal properties are systematically identified, and the vibration modes are classified into rotational, translational, planet and purely ring modes. The well-defined properties of each mode type provide a crucial foundation for the current problem of parametric instability with an elastically deformable ring gear.

Parametric instability in single-pair gears has been investigated in [16-19]. Only a few studies exist on parametric instabilities of multiple mesh gear systems. Tordion and Gauvin [20] and Benton and Seireg [21] analyzed the instabilities of two-stage gear systems but with contradictory conclusions. This was clarified by Lin and Parker [22], who derived formulae that allow designers to suppress particular instabilities by choice of contact ratios and mesh phasing. Liu and Parker [23] analytically investigated the nonlinear resonant vibration of idler gears parametrically excited by mesh stiffness variation. The impact of mesh stiffness variation on tooth loads and load sharing in planetary gears was studied by August and Kasuba [6] and Velex and Flamand [24]. They numerically computed the dynamic response of planetary gears with three sequentially phased meshes and found the impact of mesh stiffness variations on dynamic response is significant. Lin and Parker [25] analytically investigated the parametric instability of planetary gears using a purely rotational model, and Bahk and Parker [26] extend this to examine the nonlinear dynamics. All of these works adopt a rigid ring model.

This work examines planetary gear parametric instability using a model that includes the translational vibration of all components and the elastic deformation of the ring gear. With the modal expressions of the elastic-discrete model from [3], the instability

 Copyright © 2009 by ASME

boundaries are obtained as simple expressions. We show that many modes can not interact to create combination instabilities, and general instability existence rules are obtained for equally spaced planets. By adjusting the tooth numbers, contact ratios, and mesh phase one can minimize or completely suppress many potential instabilities.

NOMENCLATURE

Ω	Mesh frequency	k_j, k_{ju}	Translational and rotational stiffness of supports/bearing for the carrier and sun, $j = c, s$
α_s	Pressure angle of sun-planet mesh	k_{bend}	Ring bending stiffness
α_r	Pressure angle of ring-planet mesh	k_{sp}	Sun-planet mesh stiffness
ψ_n	Location of the n^{th} planet	k_{rp}	Ring-planet mesh stiffness
ψ_{rn}	$= \psi_n + \alpha_r$	k_{rbs}, k_{rus}	Radial, tangential distributed ring foundation stiffnesses
ψ_{sn}	$= \psi_n - \alpha_s$	I_j	Moment of inertia of the ring, carrier and sun, $j = r, c, s$
γ_{sr}	Mesh phase between sun-planet and ring-planet mesh	m_j	Mass of the ring, carrier and sun, $j = r, c, s$
ν	Poisson's ratio	r_j	Base radius for the ring, carrier and sun, $j = r, c, s$
E	Young's modulus	r_1, r_2	Inner, outer radii of the ring gear
J	Area moment of inertia	u, w	Ring tangential, radial deflections
N	Number of planets	v	Ring elastic tangential deflection
R	Pitch radius of the ring gear	x_j, y_j, u_j	Translational and rotational displacements of the ring, carrier and sun, $j = r, c, s$
c_s, c_r	Contact ratios of sun-planet and ring-planet meshes	ξ_n, η_n, u_n	Radial, tangential, and rotational displacements of the n^{th} planet
k_{pn}	n^{th} planet bearing stiffness	z_s, z_r	Tooth numbers of the sun and ring

MATHEMATICAL FORMULATION

Figure 1 shows the elastic-discrete model of a planetary gear. The ring gear is modeled as a thin elastic body, and the sun, carrier and planets are treated as rigid bodies. The elastic-discrete model is established in detail in [3]. The same dimensionless parameters as in [3] are adopted here. The symbols with $\sim$ are dimensional variables, and the same symbols are used for dimensionless variables but without the $\sim$.

The degrees of freedom and dimensionless quantities are (also see the Appendix)

$$v = \frac{\tilde{v}}{R}, \quad \mathbf{q} = \frac{\tilde{\mathbf{q}}}{R},$$
$$\tilde{\mathbf{q}} = [\underbrace{\tilde{x}_r, \tilde{y}_r, \tilde{u}_r}_{\mathbf{p}_r}, \underbrace{\tilde{x}_c, \tilde{y}_c, \tilde{u}_c}_{\mathbf{p}_c}, \underbrace{\tilde{x}_s, \tilde{y}_s, \tilde{u}_s}_{\mathbf{p}_s}, \underbrace{\tilde{\xi}_1, \tilde{\eta}_1, \tilde{u}_1}_{\mathbf{p}_1}, \cdots, \underbrace{\tilde{\xi}_N, \tilde{\eta}_N, \tilde{u}_N}_{\mathbf{p}_N}]^T \quad (1)$$

$$\tau = \frac{t}{T}, \quad T = \sqrt{\frac{\tilde{m}_r}{\tilde{k}_{rn}}}, \quad k_i = \frac{\tilde{k}_i}{\tilde{k}_{rp}}, \; i = c, s, pn, rp, sp, bend,$$
$$k_{rbs} = \frac{\tilde{k}_{rbs} R}{\tilde{k}_{rp}}, \quad k_{rus} = \frac{\tilde{k}_{rus} R}{\tilde{k}_{rp}}, \quad (2)$$

$$k_{bend} = \frac{EJ}{\tilde{k}_{rp} R^3 (1 - \nu^2)}, \quad m_j = \frac{\tilde{m}_j}{\tilde{m}_r}, \quad I_j = \frac{\tilde{I}_j}{\tilde{m}_r r_j^2}, \quad j = r, c, s, n,$$
$$\mathbf{M}_i = \frac{\tilde{\mathbf{M}}_i}{\tilde{m}_r}, \quad i = r, c, s, n, \quad (3)$$

$$\mathbf{K}_j = \frac{\tilde{\mathbf{K}}_j}{\tilde{k}_{rp}}, \quad j = rb, cb, sb, pp, \quad \mathbf{K}_i^n = \frac{\tilde{\mathbf{K}}_i^n}{\tilde{k}_{rp}},$$
$$i = r1, r2, c1, c2, s1, s2. \quad (4)$$

Above and in what follows, N is the number of planets; $n = 1, \cdots, N$ is the planet index; x_h, y_h, $h = r, c, s$ are the translations of the ring rigid motion, carrier and sun; ξ_n, η_n are the radial

Copyright © 2009 by ASME

and tangential translations of the planets; and $u_h = r_h\theta_h$, where $h = r, c, s, 1, \cdots, N$ are rotational deflections (rotation in radians times the gear base radii r_r, r_s, r_p or radius of the carrier r_c). Subsequently, all parameters are dimensionless.

The motion of the ring $u(\theta,t)$ is separated into two parts: the rigid body motion (x_r, y_r, u_r) and the elastic tangential deformation $v(\theta,t)$, which is related to the elastic radial deflection by the inextensibility condition $w(\theta,t) = -\partial v(\theta,t)/\partial\theta$.

The bearings and supports of each of the sun, carrier and planets are modeled as two perpendicular springs with equal stiffness, while the bearings and supports of the ring gear are represented by an elastic foundation with distributed tangential and radial stiffnesses. All planets are identical and equally spaced, and all planet bearing stiffnesses are equal. The sun-planet and ring-planet tooth meshes are modeled as springs with time-varying stiffnesses.

The time-varying sun-planet and ring-planet mesh stiffnesses for the n^{th} planet are

$$k_{sn}(t) = k_{sp} + k_{1n}(t), \quad k_{rn}(t) = k_{rp} + k_{2n}(t) = 1 + k_{2n}(t), \quad (5)$$

where $k_{sp} = O(1)$ and $k_{rp} = 1$ (a result of non-dimensionalization) are mean values. $k_{1n}(t)$, $k_{2n}(t)$ are the zero-mean mesh stiffness variations as the number of tooth pairs in contact changes for the sun-planet and ring planet meshes. Rectangular waves as in Figure 2 approximate the mesh stiffness variations. Fourier expansion of the mesh stiffness variations $k_{1n}(t)$ and $k_{2n}(t)$ gives

$$\begin{aligned} k_{1n}(t) &= 2\mu \sum_{L=1}^{\infty} [a_{sn}^{(L)} \sin L\Omega t + b_{sn}^{(L)} \cos L\Omega t], \\ k_{2n}(t) &= 2\varepsilon \sum_{L=1}^{\infty} [a_{rn}^{(L)} \sin L\Omega t + b_{rn}^{(L)} \cos L\Omega t], \end{aligned} \quad (6)$$

$$\begin{aligned} a_{sn}^{(L)} &= \frac{2}{L\pi} \sin[L\pi(c_s + 2\gamma_{sn})] \sin(L\pi c_s), \\ b_{sn}^{(L)} &= \frac{2}{L\pi} \cos[L\pi(c_s + 2\gamma_{sn})] \sin(L\pi c_s), \end{aligned} \quad (7)$$

$$\begin{aligned} a_{rn}^{(L)} &= \frac{2}{L\pi} \sin[L\pi(c_r + 2\gamma_{sn} + 2\gamma_{sr})] \sin(L\pi c_r), \\ b_{rn}^{(L)} &= \frac{2}{L\pi} \cos[L\pi(c_r + 2\gamma_{sn} + 2\gamma_{sr})] \sin(L\pi c_r), \end{aligned} \quad (8)$$

where 2μ and 2ε are peak-to-peak values of $k_{1n}(t)$ and $k_{2n}(t)$, respectively, c_s and c_r are contact ratios of the sun-planet and ring-planet meshes, and Ω is the mesh frequency. The phases of $k_{1n}(t)$ and $k_{2n}(t)$ are γ_{sn} and $\gamma_{rn} = \gamma_{sn} + \gamma_{sr}$, where γ_{sn} is the phase of the n^{th} sun-planet mesh and γ_{sr} is the mesh phase between the sun-planet and ring-planet meshes for a given planet, which is the same for each planet [22, 27]. Note that $\gamma_{s1} = 0$.

The displacement of the whole system $\mathbf{a}$ is the combination of the elastic deformation of the ring $v(\theta,t)$ and the discrete body deflections $\mathbf{q}$ as

$$\mathbf{a}^T = [v, \mathbf{q}^T]. \quad (9)$$

Based on the equations of motion for the time-invariant system [3], the dimensionless equation of motion for the time-varying system is

$$M\ddot{\mathbf{a}} + K(t)\mathbf{a} = 0, \quad (10)$$

where M and $K(t)$are extended inertia and stiffness operators defined in the Appendix. M and $K(t)$ are the same operators as M,K in [3] with k_{sn}, k_{rn} in K substituted by the time-varying mesh stiffnesses $k_{sn}(t)$, $k_{rn}(t)$. M and $K(t)$ are self-adjoint with the inner product $< \mathbf{a}^1, \mathbf{a}^2 >= \int_0^{2\pi} v^1 \bar{v}^2 d\theta + (\mathbf{q}^1)^T \bar{\mathbf{q}}^2$, where the overbar denotes complex conjugation.

The ratios of the amplitudes of sun-planet and ring-planet mesh stiffness variations to their mean values are μ/k_{sp} and ε, respectively. We assume μ/k_{sp} is of the same order as ε, i.e., $\mu/k_{sp} = g\varepsilon$, where $g = O(1)$. The extended stiffness operator $K(t)$ is separated into time-varying and time-invariant parts as

$$K(t) = K_0 + 2\varepsilon \sum_{L=1}^{\infty} [K_{v1}^{(L)} \sin L\Omega t + K_{v2}^{(L)} \cos L\Omega t], \quad (11)$$

where K_0 is the stiffness operator for the time-invariant system, which has the same form as $K(t)$with $k_{sn}(t)$, $k_{rn}(t)$ substituted by k_{sp} and 1, respectively. The Fourier coefficient operators $K_{v1}^{(L)}$ and $K_{v2}^{(L)}$ also have the same form as $K(t)$ with the following substitutions. For $K_{v1}^{(L)}$, the mesh stiffnesses $k_{sn}(t)$, $k_{rn}(t)$ in $K(t)$are substituted by $k_{sp} g a_{sn}^{(L)}$, $a_{rn}^{(L)}$. For $K_{v2}^{(L)}$, the mesh stiffnesses $k_{sn}(t)$, $k_{rn}(t)$ in $K(t)$are substituted by $k_{sp} g b_{sn}^{(L)}$, $b_{rn}^{(L)}$.

The method of multiple scales is used with the introduction of the slow time $\tau = \varepsilon t$, and the dynamic response is represented as

$$\mathbf{a} = \mathbf{a}_0(t,\tau) + \varepsilon \mathbf{a}_1(t,\tau) + O(\varepsilon^2), \quad \mathbf{a}_0 = \begin{bmatrix} v_0 \\ \mathbf{q}_0 \end{bmatrix}, \quad \mathbf{a}_1 = \begin{bmatrix} v_1 \\ \mathbf{q}_1 \end{bmatrix}. \quad (12)$$

Substitution of (12) into (10), use of $\frac{d}{dt} \rightarrow \frac{\partial}{\partial t} + \varepsilon \frac{\partial}{\partial \tau}$, and separation of powers in ε lead to

$$M \frac{\partial^2 \mathbf{a}_0}{\partial t^2} + K_0 \mathbf{a}_0 = \mathbf{0}, \quad (13)$$

Copyright © 2009 by ASME

$$
\begin{aligned}
&M\frac{\partial^2 \mathbf{a}_1}{\partial t^2}+K_0\mathbf{a}_1=-2M\frac{\partial^2 \mathbf{a}_0}{\partial t\partial\tau}- \\
&2\sum_{L=1}^{\infty}(K_{v1}^{(L)}\sin L\Omega t+K_{v2}^{(L)}\cos L\Omega t)\mathbf{a}_0
\end{aligned}. \tag{14}
$$

The general solution for the time-invariant system (13) is

$$
\mathbf{a}_0=\sum_{s=1}^{\infty}c_s(\tau)\mathbf{Y_s}(\theta)e^{i\omega_s t}+c.c., \tag{15}
$$

where $\mathbf{Y_s}(\theta)$ are the eigenfunctions in extended variable form and $c.c.$ refers to the complex conjugate of preceding terms. The natural modes $\mathbf{Y_s}(\theta)$ in (15) are analytically solved by Wu and Parker [3]. The multiplicity of the natural frequencies ω_s are summarized as: (i) Rotational and purely ring modes have distinct natural frequencies; (ii) Translational modes are degenerate with multiplicity two; and (iii) If the number of planets is odd, all the planet modes are degenerate with multiplicity two, otherwise, the planet modes may be either degenerate with multiplicity two or distinct; note that planet modes exist only when the number of planets $N \geqslant 4$. Therefore, all natural frequencies of planetary gears with an elastic ring gear are either distinct or degenerate with multiplicity two.

When a harmonic of the mesh frequency is close to the sum of two natural frequencies secular terms exist in (14), which leads to sum type parametric instability. This condition is

$$
L\Omega=\omega_p+\omega_q+\varepsilon\sigma. \tag{16}
$$

where $\sigma=O(1)$ is a detuning parameter. When a harmonic of mesh frequency is close to the difference of two natural frequencies, such as $L\Omega=\omega_p-\omega_q+\varepsilon\sigma$, one can show that difference type parametric instabilities are not possible. According to the degeneracy of ω_p and ω_q , the solvability conditions of (14) are classified into three cases: Case 1, both eigenvalues are distinct; Case 2, one eigenvalue is distinct and the other is degenerate; Case 3, both eigenvalues are degenerate. Single mode instabilities are treated as a special case of combination instabilities with $\omega_p=\omega_q$.

Case 1: Instability boundaries for two distinct eigenvalues

Consider the case where ω_p and ω_q are distinct natural frequencies. When (15) is used in (14) and condition (16) is invoked, the two solvability conditions of (14) for $s=p$ and $s=q$ are

$$
\begin{aligned}
&i2\omega_p\frac{\partial c_p}{\partial\tau}+(E_{pq}^{(L)}-iD_{pq}^{(L)})\bar{c}_q e^{i\sigma\tau}=0,\\
&i2\omega_q\frac{\partial c_q}{\partial\tau}+(E_{qp}^{(L)}-iD_{qp}^{(L)})\bar{c}_p e^{i\sigma\tau}=0,
\end{aligned} \tag{17}
$$

$$
\begin{aligned}
D_{pq}^{(L)}&=D_{qp}^{(L)}=<\mathbf{Y}_p,K_{v1}^{(L)}\mathbf{Y}_q>,\\
E_{pq}^{(L)}&=E_{qp}^{(L)}=<\mathbf{Y}_p,K_{v2}^{(L)}\mathbf{Y}_q>,
\end{aligned} \tag{18}
$$

where $D_{pq}^{(L)}=D_{qp}^{(L)}$ and $E_{pq}^{(L)}=E_{qp}^{(L)}$. For all $s\neq p,q$ in (15), the solvability conditions of (14) lead to $c_s(\tau)=$constant (and $c_s(\tau)=0$ if any damping is present) . The solutions of (17) are bounded only when

$$
\sigma\geqslant\sqrt{\Lambda_{pq}^{(L)}/(\omega_p\omega_q)}, \tag{19}
$$

$$
\Lambda_{pq}^{(L)}=D_{pq}^{(L)}D_{qp}^{(L)}+E_{pq}^{(L)}E_{qp}^{(L)}=\left(D_{pq}^{(L)}\right)^2+\left(E_{pq}^{(L)}\right)^2. \tag{20}
$$

The instability boundaries for two distinct natural frequency modes are thus:

Combination instabilities:

$$
\Omega=\frac{\omega_p+\omega_q}{L}\pm\frac{\varepsilon}{L}\sqrt{\Lambda_{pq}^{(L)}/(\omega_p\omega_q)} \tag{21}
$$

Single mode instabilities:

$$
\Omega=\frac{2\omega_p}{L}\pm\frac{\varepsilon}{L\omega_p}\sqrt{\Lambda_{pp}^{(L)}} \tag{22}
$$

Case 2: Instability boundaries for distinct-degenerate eigenvalues

If one of the natural frequencies in (16) is degenerate with multiplicity two (such as $\omega_q=\omega_m$) and the other remains distinct, the solvability conditions of (14) generate three equations. With some algebraic manipulation, the combination instability boundaries for modes with distinct-degenerate eigenvalues are obtained in closed-form as in (21) with

$$
\Lambda_{pq}^{(L)}=\left(D_{pq}^{(L)}\right)^2+\left(D_{pm}^{(L)}\right)^2+\left(E_{pq}^{(L)}\right)^2+\left(E_{pm}^{(L)}\right)^2. \tag{23}
$$

Case 3: Instability boundaries for two degenerate eigenvalues

When both natural frequencies in (16) are degenerate such that $\omega_p=\omega_q$ and $\omega_r=\omega_m$, the solvability conditions of (14) generate four equations. Due to the size of the coefficient matrix, the instability boundaries can not be expressed in simple expressions unless one finds simplifying properties of $D_{pq}^{(L)}$, $E_{pq}^{(L)}$, $D_{pm}^{(L)}$, $E_{pm}^{(L)},\cdots$.

All three cases above require further analysis of $D_{pq}^{(L)}$ and $E_{pq}^{(L)}$ in (18), which expand to give

$$
D_{pq}^{(L)}=k_{sp}g\sum_{n=1}^{N}a_{sn}^{(L)}\delta_{sn}^{[p]}\delta_{sn}^{[q]}+\sum_{n=1}^{N}a_{rn}^{(L)}\delta_{rn}^{[p]}\delta_{rn}^{[q]}, \tag{24}
$$

Copyright © 2009 by ASME

$$E_{pq}^{(L)} = k_{sp} g \sum_{n=1}^{N} b_{sn}^{(L)} \delta_{sn}^{[p]} \delta_{sn}^{[q]} + \sum_{n=1}^{N} b_{rn}^{(L)} \delta_{rn}^{[p]} \delta_{rn}^{[q]}, \qquad (25)$$

$$\begin{array}{l} \delta_{sn}^{[p]} = y_s \cos\psi_{sn} - x_s \sin\psi_{sn} - \xi_n \sin\alpha_s - \eta_n \cos\alpha_s \\ +u_s + u_n \end{array}, \qquad (26)$$

$$\begin{array}{l} \delta_{rn}^{[p]} = \left(v\cos\alpha_r + \frac{\partial v}{\partial\theta}\sin\alpha_r\right)\Big|_{\theta=\psi_n} - x_r \sin\psi_{rn} + \\ y_r \cos\psi_{rn} + u_r + \xi_n \sin\alpha_r - \eta_n \cos\alpha_r - u_n \end{array}. \qquad (27)$$

where $\delta_{sn}^{[p]}$ and $\delta_{rn}^{[p]}$ are deformations of the n^{th} sun-planet and ring-planet meshes for the p^{th} mode, α_s and α_r are the pressure angles of the sun-planet and ring-planet meshes, and $\psi_{sn} = \psi_n - \alpha_s$, $\psi_{rn} = \psi_n + \alpha_r$, where $\psi_n = 2\pi(n-1)/N$ is the circumferential planet location. From (24) and (25), $D_{pq}^{(L)}$ and $E_{pq}^{(L)}$ depend on modal gear mesh deformations and the Fourier coefficients of the mesh stiffness variations.

MODAL PROPERTIES AND GEAR MESH DEFORMATIONS

Fourier expansion of the elastic deflection of the ring gives

$$v(\theta) = \sum_{m=\pm 2}^{\pm JN} V_m e^{im\theta}, \qquad (28)$$

where $J \geqslant 1$ is an arbitrarily large integer. For all vibration modes, the deformations of the ring-planet and sun-planet meshes are expressed in a general compact form as

$$\delta_{jn} = c_1 \cos T\psi_n + c_2 \sin T\psi_n, \quad j = s, r, \qquad (29)$$

where c_1 and c_2 are coefficients independent of ψ_n, and T is an integer to be determined for each type of mode (i.e., rotational , translational, planet and purely ring modes). A mesh deformation having the form (29) is called type T deformation. For each type of mode, T is determined below.

A rotational mode (mode p) in extended variable form has the structure [3]

$$\mathbf{a}^{[p]} = \left[\sum_{m=1}^{J} \left[(\cos\alpha_r - imN\sin\alpha_r)e^{imN\theta} + c.c.\right] V_m^{[p]}, \mathbf{q}_{rot}^T\right]^T, \qquad (30)$$

$$\begin{array}{l} \mathbf{q}_{rot} = [0, 0, u_r^{[p]}, 0, 0, u_c^{[p]} 0, 0, u_s^{[p]}, \xi_1^{[p]}, \eta_1^{[p]}, u_1^{[p]}, \\ \cdots, \xi_1^{[p]}, \eta_1^{[p]}, u_1^{[p]}]^T \end{array}, \qquad (31)$$

where the $V_m^{[p]}$ are real. According to (30) and (31), the translations of the sun, carrier and ring rigid motion are zero, the displacements of all planets are identical, and the elastic deflection of the ring is a linear combination of the mN nodal diameter components. With these properties, substitution of (31) into (26) ensures $\delta_{sn}^{[p]}$ is independent of ψ_n as

$$\delta_{sn}^{[p]} = \delta_{s1}^{[p]} = -\xi_1^{[p]} \sin\alpha_s - \eta_1^{[p]} \cos\alpha_s + u_1^{[p]} + u_s^{[p]}. \qquad (32)$$

Similarly, $\delta_{rn}^{[p]}$ is independent of ψ_n due to the modal properties and the identities $\cos lN\psi_n = 1$ and $\sin lN\psi_n = 0$,

$$\begin{array}{l} \delta_{rn}^{[p]} = \delta_{r1}^{[p]} = \sum\limits_{l=1}^{\infty} 2U_m(\cos^2\alpha_r + m^2 \sin^2\alpha_r) + u_r^{[p]} \\ +\xi_1^{[p]} \sin\alpha_r - \eta_1^{[p]} \cos\alpha_r - u_1^{[p]} \end{array}. \qquad (33)$$

$\delta_{sn}^{[p]}$ and $\delta_{rn}^{[p]}$ in (32) and (33) have the form of (29) with $T = 0$. Accordingly, they are called type 0 deformations.

Similarly, one can show that $T = 1$ for translational modes (they are called type 1 deformations). Therefore, for a pair of type d planet modes in (**??**)-(**??**), the sun-planet and ring-planet mesh deflections are type d deformations as defined in (29). These results are for any N. When N is even, extra distinct planet modes exist. They have the form of (**??**) with $d = N/2$. The corresponding gear mesh deformations are of type $N/2$.

The sun-planet and ring-planet mesh deformations of purely ring modes are zero. For a purely ring mode p, $D_{pq}^{(L)}$**,** $E_{pq}^{(L)}$ in (24) and (25) always vanish because the gear mesh deflections are zero. Thus, combination and single mode instabilities associated with a purely ring mode in (20)-(23) and (23) *always* vanish.

PARAMETRIC INSTABILITIES FOR IN-PHASE MESHES

Equal planet spacing requires $(z_s + z_r)/N$ to be an integer, where z_s and z_r are the tooth numbers of the sun and ring. The gear mesh phases [27] are defined as $\gamma_{sn} = (n-1)z_s/N$ for clockwise planet rotation. When z_s and z_r are both integer multiples of N, all of the sun-planet meshes are in-phase ($\gamma_{sn} = 0$) and all the ring-planet meshes are in-phase.

Parametric Instabilities for In-Phase Meshes

For in-phase planet meshes, the Fourier coefficients of the mesh stiffness variations in (7) and (8) are independent of the planet index n [28], so $a_{sn}^{(L)}$,$a_{rn}^{(L)}$, $b_{sn}^{(L)}$, $b_{rn}^{(L)}$ in (24) and (25) are moved outside of the summations to give

$$D_{pq}^{(L)} = k_{sp} g a_{s1}^{(L)} \sum_{n=1}^{N} \delta_{sn}^{[p]} \delta_{sn}^{[q]} + a_{r1}^{(L)} \sum_{n=1}^{N} \delta_{rn}^{[p]} \delta_{rn}^{[q]}, \qquad (34)$$

Copyright © 2009 by ASME

$$E_{pq}^{(L)} = k_{sp} g b_{s1}^{(L)} \sum_{n=1}^{N} \delta_{sn}^{[p]} \delta_{sn}^{[q]} + b_{r1}^{(L)} \sum_{n=1}^{N} \delta_{rn}^{[p]} \delta_{rn}^{[q]}. \quad (35)$$

With the general expression of the mesh deflection in (29), the summation terms in (34) and (35) are written as

$$\sum_{n=1}^{N} \delta_{jn}^{[p]} \delta_{jn}^{[q]} = \sum_{n=1}^{N} (c_1 \cos T_p \psi_n + c_2 \sin T_p \psi_n) (c_3 \cos T_q \psi_n + c_4 \sin T_q \psi_n), \quad j = s,\ r, \quad (36)$$

where c_i, $i = 1,2,3,4$ are known coefficients for the given modes p and q. T_p and T_q are indices of mesh deformation types for modes p and $q$as defined in (29).

For equally spaced planets, the following identities hold for integer l

$$\sum_{n=1}^{N} \sin T_p \psi_n \sin T_q \psi_n = \sum_{n=1}^{N} \sin T_p \psi_n \cos T_q \psi_n = \sum_{n=1}^{N} \cos T_p \psi_n \cos T_q \psi_n = 0,$$

for any

$$T_p \pm T_q \neq lN \quad (37)$$

For all types of modes, T_p and T_q are integers within $[0, int(N/2)]$, so the condition $T_p \pm T_q \neq lN$ in (62) is equivalent to $T_p \neq T_q$. Three cases must be considered:

1. When $T_p \neq T_q$, $D_{pq}^{(L)} = E_{pq}^{(L)} = 0$ according to (34), (35), (36) and (62). Thus, for any potential distinct-distinct instability with $T_p \neq T_q$, $\Lambda_{pq}^{(L)}$ in (20) vanishes, which ensures that no such instability is possible. For example, no combination instability can occur between a rotational mode and a distinct planet mode.
2. For distinct-degenerate combination instabilities, it is always the case that $T_p \neq T_q$ and $T_m = T_q$, from which $D_{pq}^{(L)}$, $E_{pq}^{(L)}$, $D_{pm}^{(L)}$, $E_{pm}^{(L)}$ in (23) vanish and so does $\Lambda_{pq}^{(L)}$; no distinct-degenerate instabilities occur. As one example, combination instabilities between a rotational mode and any pair of translational modes can not occur.
3. For degenerate-degenerate instabilities where $T_p \neq T_r$ (and, of course, $T_q = T_p$, $T_m = T_r$), all terms associated with $D_{pr}^{(L)}$, $E_{pr}^{(L)}$, $D_{pm}^{(L)}$, $E_{pm}^{(L)}$, $\cdots$ in (**??**)-(**??**) vanish, and so do these combination instabilities. Thus, degenerate-degenerate instabilities can occur only between two degenerate pairs of the same type (i.e, two pairs of translational modes, or two pairs of planet modes).

Therefore, one can state a key rule governing the existence or elimination of parametric instabilities for in-phase meshes: If two modes have the same type of gear mesh deformation their combination instability exists, otherwise their combination instability vanishes. This result is independent of which mesh frequency harmonic L is the source of potential instability (see (16)).

Consequently, all distinct-degenerate instabilities vanish for in-phase planet meshes. The following sections examine the remaining cases of distinct-distinct and degenerate-degenerate instabilities that do not vanish.

Distinct-Distinct Combination Instabilities for In-Phase Meshes The possible distinct-distinct combination instabilities involve rotational, purely ring and distinct planet modes. As shown above, however, all distinct-distinct instability boundaries vanish for in-phase meshes except for two cases: (a) two rotational modes; (b) two distinct planet modes.

For both cases of distinct-distinct combination instability, reduction of (20), (24) and (25) using the properties of each mode type yield a common form defining the instability boundaries as

$$\varepsilon^2 \Lambda_{pq}^{(L)} = \frac{4N^2}{L^2\pi^2} [\mu^2 (\delta_{s1}^{[p]} \delta_{s1}^{[q]})^2 \sin^2(L\pi c_s) + \varepsilon^2 (\delta_{r1}^{[p]} \delta_{r1}^{[q]})^2 \sin^2(L\pi c_r) + 2\mu\varepsilon \delta_{s1}^{[p]} \delta_{r1}^{[p]} \delta_{s1}^{[q]} \delta_{r1}^{[q]} \sin(L\pi c_s) \sin(L\pi c_r) \cos L\pi(c_r + 2\gamma_{sr} - c_s)] \quad (38)$$

For two rotational modes, $\delta_{s1}^{[p]}$, $\delta_{s1}^{[q]}$, $\delta_{r1}^{[p]}$, $\delta_{r1}^{[q]}$ in (38) are given by (32) and (33). For two distinct planet modes, they are given by (**??**)-(**??**). Distinct planet modes exist only for even N, and substitution of $d = N/2$ into (**??**) and (**??**) yields expressions for the n^{th} mesh deflections in terms of the first mesh deflections

$$\delta_{sn}^{[p]} = (-1)^n \delta_{s1}^{[p]}, \quad \delta_{rn}^{[p]} = (-1)^n \delta_{r1}^{[p]}, \quad \delta_{sn}^{[q]} = (-1)^n \delta_{s1}^{[q]}, \quad \delta_{rn}^{[q]} = (-1)^n \delta_{r1}^{[q]}. \quad (39)$$

Equation (39) indicates that the product of two mesh deflections is independent of n, which is needed to establish (38) as the instability boundary for this case.

The contact ratios c_s, c_r and the phase difference between the sun-planet and ring-planet meshes γ_{sr} are governed by the gear geometries. The expression for γ_{sr} is given in [28]. When both Lc_s and Lc_r are integers, all potential instabilities driven by the L^{th} harmonic of mesh frequency vanish. When neither of Lc_s, Lc_r are integers, a minimum instability region can be achieved by adjusting c_s, c_r and γ_{sr} in the third term of (38) such that this term is negative with absolute value comparable to the sum of the first two terms. For any two given modes, the sign of $\delta_{s1}^{[p]} \delta_{r1}^{[p]} \delta_{s1}^{[q]} \delta_{r1}^{[q]}$ in (38) is unambiguous because multiplication of a mode by -1 does not change the products $\delta_{s1}^{[p]} \delta_{r1}^{[p]}$ and $\delta_{s1}^{[q]} \delta_{r1}^{[q]}$. According to (22), the width of the instability region of two distinct modes is $\Delta\Omega = \frac{2}{L}\sqrt{\varepsilon^2 \Lambda_{pq}^{(L)} / (\omega_p \omega_q)}$, which is proportional to the number of planets N and inversely proportional to L^2.

Copyright © 2009 by ASME

Degenerate-Degenerate Combination Instabilities for In-Phase Meshes According to the instability existence rule for in-phase meshes, combination instabilities between a pair of translational modes and a pair of degenerate planet modes always vanish because they have different mesh deformations as defined in (29). Combination instabilities for degenerate modes exist only between two pairs of translational modes or between two pairs of type d planet modes. Closed-form expressions of instability boundaries for two pairs of degenerate modes are obtained as follows.

For two degenerate translational mode pairs such as $\omega_p = \omega_q$ and $\omega_r = \omega_m$, $\delta_{sn}^{[p]}$ and $\delta_{sn}^{[q]}$ are determined by (**??**) and $\delta_{sn}^{[r]}$, $\delta_{sn}^{[m]}$ are given by analogous expressions. According to (**??**) and (62), the following equations hold

$$\sum_{n=1}^{N} \delta_{jn}^{[p]} \delta_{jn}^{[r]} = \sum_{n=1}^{N} \delta_{jn}^{[q]} \delta_{jn}^{[m]}, \quad \sum_{n=1}^{N} \delta_{jn}^{[p]} \delta_{jn}^{[m]} = -\sum_{n=1}^{N} \delta_{jn}^{[q]} \delta_{jn}^{[r]}, \quad j = s, r. \tag{40}$$

Substitution of (40) into (24) and (25) gives

$$D_{pr} = D_{qm}, \quad E_{pr} = E_{qm}, \quad D_{pm} = -D_{qr}, \quad E_{pm} = -E_{qr}. \tag{41}$$

Substitution of (41) into the coefficient matrix of (**??**)-(**??**) yields a simple expression for the 8×8 eigenvalue problem. Requiring the eigenvalues of the coefficient matrix to have non-positive real parts yields two overlapping sets of combination instability boundaries, where one set envelops the other and so bounds the full instability region. The instability region boundaries are thus

$$\Omega = (\omega_p + \omega_r)/L \pm \sqrt{\varepsilon^2 \Gamma_{pr}^{(L)}/(\omega_p \omega_r)}/L, \quad \Gamma_{pr}^{(L)} = \max(\Delta_1^{(L)}, \Delta_2^{(L)}), \tag{42}$$

$$\begin{aligned} \Delta_1^{(L)} &= (D_{pr}^{(L)} - E_{pm}^{(L)})^2 + (D_{pm}^{(L)} + E_{pr}^{(L)})^2, \\ \Delta_2^{(L)} &= (D_{pr}^{(L)} + E_{pm}^{(L)})^2 + (D_{pm}^{(L)} - E_{pr}^{(L)})^2. \end{aligned} \tag{43}$$

With the properties of gear mesh deformations in (**??**), $\Delta_1^{(L)}$ and $\Delta_2^{(L)}$ for two translational modes are written in terms of the mesh parameters as

$$\begin{aligned} \begin{matrix} \varepsilon^2 \Delta_1^{(L)} \\ \varepsilon^2 \Delta_2^{(L)} \end{matrix} &= \tfrac{N^2}{L^2 \pi^2} \left\{ (\beta_1^2 + \beta_3^2) \sin^2(L\pi c_s) + (\beta_2^2 + \beta_4^2) \right. \\ & \sin^2(L\pi c_r) + 2 \sin(L\pi c_s) \sin(L\pi c_r) \\ & \cdot [(\beta_1 \beta_2 + \beta_3 \beta_4) \cos L\pi(c_r + 2\gamma_{sr} - c_s) \\ & \left. \pm (\beta_1 \beta_4 - \beta_2 \beta_3) \sin L\pi(c_r + 2\gamma_{sr} - c_s)] \right\}, \end{aligned} \tag{44}$$

$$\beta_1 = \mu(\delta_{s1}^{[p]} \delta_{s1}^{[r]} + \delta_{s1}^{[q]} \delta_{s1}^{[m]}), \quad \beta_2 = \varepsilon(\delta_{r1}^{[p]} \delta_{r1}^{[r]} + \delta_{r1}^{[q]} \delta_{r1}^{[m]}), \tag{45}$$

$$\beta_3 = \mu(\delta_{s1}^{[p]} \delta_{s1}^{[m]} - \delta_{s1}^{[r]} \delta_{s1}^{[q]}), \quad \beta_4 = \varepsilon(\delta_{r1}^{[p]} \delta_{r1}^{[m]} - \delta_{r1}^{[r]} \delta_{r1}^{[q]}), \tag{46}$$

where the gear mesh deflections $\delta_{s1}^{[p]}$, $\delta_{s1}^{[q]}$, $\delta_{r1}^{[p]}$, $\delta_{r1}^{[q]}$ are governed by (**??**)-(**??**) (with similar equations for modes r and m). The instability boundaries for a single pair of translational modes are obtained by the replacements $r \to p$ and $m \to q$ in (45)-(46) to give

$$\begin{aligned} \begin{matrix} \varepsilon^2 \Delta_1^{(L)} \\ \varepsilon^2 \Delta_2^{(L)} \end{matrix} &= \tfrac{N^2}{L^2 \pi^2} [\beta_1^2 \sin^2(L\pi c_s) + \beta_2^2 \sin^2(L\pi c_r) +, \\ & 2\beta_1 \beta_2 \sin(L\pi c_s) \sin(L\pi c_r) \cos L\pi(c_r + 2\gamma_{sr} - c_s)] \end{aligned} \tag{47}$$

with $\beta_1 = \mu \left[(\delta_{s1}^{[p]})^2 + (\delta_{s1}^{[q]})^2 \right]$, $\beta_2 = \varepsilon \left[(\delta_{r1}^{[p]})^2 + (\delta_{r1}^{[q]})^2 \right]$. Similarly, for two pairs of degenerate planet modes of the same type, the same properties as (40)-(41) are found. Therefore, the instability boundaries of two pairs of type d planet modes are also governed by (42)-(43). With the properties of gear mesh deformations, $\Delta_1^{(L)}$ and $\Delta_2^{(L)}$ for two pairs of planet modes of the same type governed by (**??**) and (**??**) simplify to

$$\begin{aligned} \begin{matrix} \varepsilon^2 \Delta_1^{(L)} \\ \varepsilon^2 \Delta_2^{(L)} \end{matrix} &= \frac{N^2}{L^2 \pi^2} \left\{ \beta_5^2 \sin^2(L\pi c_s) + (\beta_6^2 + \beta_7^2) \sin^2(L\pi c_r) \right. \\ & + 2\beta_5 \sin(L\pi c_s) \sin(L\pi c_r) \cdot [\beta_6 \cos L\pi(c_r + 2\gamma_{sr} - c_s) \\ & \left. \pm \beta_7 \sin L\pi(c_r + 2\gamma_{sr} - c_s) \,] \right\}, \end{aligned} \tag{48}$$

$$\beta_5 = \mu \delta_{s1}^{[p]} \delta_{s1}^{[r]}, \quad \beta_6 = \varepsilon(\delta_{r1}^{[p]} \delta_{r1}^{[r]} + \delta_{r1}^{[q]} \delta_{r1}^{[m]}), \quad \beta_7 = \varepsilon(\delta_{r1}^{[p]} \delta_{r1}^{[m]} - \delta_{r1}^{[q]} \delta_{r1}^{[r]}), \tag{49}$$

where the gear mesh deflections $\delta_{s1}^{[p]}$, $\delta_{r1}^{[p]}$, $\delta_{r1}^{[q]}$ are governed by (**??**)-(**??**) (with similar equations for modes r and m). The single degenerate planet mode pair instability boundaries are obtained by the replacements $r \to p$ and $m \to q$ in (48)-(49) to give

$$\begin{aligned} \begin{matrix} \varepsilon^2 \Delta_1^{(L)} \\ \varepsilon^2 \Delta_2^{(L)} \end{matrix} &= \tfrac{N^2}{L^2 \pi^2} \{ \beta_5^2 \sin^2(L\pi c_s) + \beta_6^2 \sin^2(L\pi c_r) \\ & + 2\beta_5 \beta_6 \sin(L\pi c_s) \sin(L\pi c_r) \\ & [\cos L\pi(c_r + 2\gamma_{sr} - c_s)] \} \end{aligned} \tag{50}$$

with $\beta_5 = \mu(\delta_{s1}^{[p]})^2$, $\beta_6 = \varepsilon \left[(\delta_{r1}^{[p]})^2 + (\delta_{r1}^{[q]})^2 \right]$.

Copyright © 2009 by ASME

Similar to (38), one can minimize the degenerate-degenerate instability regions by adjusting c_s, c_r and γ_{sr} based on (44), (47), (48) and (50).

Numerical Verification for In-Phase Meshes The foregoing closed-form expressions for the instability boundaries are compared to numerical solutions from Floquet theory. Figure 3 shows the instability boundaries for a planetary gear with four in-phase planet meshes. The parameters and the first 11 natural frequencies are given in Table 1. ω_3 and ω_7 are for rotational modes, ω_4 and ω_9 are for planet modes, $\omega_8$is for a purely ring mode, and the remaining natural frequencies in Table 1 are for translational modes. The numerical and analytical instability boundaries in Figure 3 match well. The seemingly larger numerical instability region near ω_5 results from a higher order instability for which the analytical solution is not shown. As can be seen from Figure 3, single mode instabilities near $\omega_5, \omega_7, \omega_9, 2\omega_4, 2\omega_5, 2\omega_7$ always exist. Combination instabilities exist only for modes with the same type of gear mesh deformation such as $\omega_1 + \omega_5$ (two translational modes), $\omega_3 + \omega_7$ (two rotational modes) and $(\omega_4 + \omega_9)/2$ (two planet modes). The predicted absence of instabilities for two modes with different types of gear mesh deformations, such as $\omega_1 + \omega_3$ and $\omega_3 + \omega_4$, is numerically verified.

CONCLUSIONS

This work analytically derives the parametric instability regions for planetary gears with equally spaced planets and an elastic continuum ring gear. For equal planet spacing, in-phase and sequentially phased mesh conditions are possible, and both phase conditions are considered. The following conclusions are obtained:

1. The possible parametric instabilities of planetary gears having an elastic ring are classified as: distinct-distinct, distinct-degenerate, and degenerate-degenerate depending on the natural frequency multiplicity of the unstable modes. Using the well defined modal properties of the elastic-discrete model, closed-formed expressions for distinct-distinct, distinct-degenerate and degenerate-degenerate instability boundaries are obtained for in-phase meshes.
2. Every mode can be classified by the nature of its mesh deformation using an integer index T_p. For any two modes, if their gear mesh deformation type indices satisfy $Lz_s \pm (T_p \pm T_q) \neq jN$ for given mesh frequency harmonic L, their combination instabilities vanish. When the gear meshes are in-phase, this simplifies such that combination instabilities for modes p and q vanish for any L if $T_p \neq T_q$ and exist for any L if $T_p = T_q$. This result generates useful design information evident by inspection of a simple formula.
3. For in-phase meshes, the instability boundaries are simple expressions in terms of the contact ratios ($c_s$and c_r), the mesh phase between the sun-planet and ring-planet meshes γ_{sr} and the modal mesh deformations. For any possible single-mode or combination instability, a minimum instability region can be achieved by adjusting the contact ratios and γ_{sr}.

REFERENCES

[1]. A. Kahraman, A. A. Kharazi, and M. Umrani, A Deformable Body Dynamic Analysis of Planetary Gears with Thin Rims, Journal of Sound and Vibration, 262 (2003), 752-768.

[2]. T. Hidaka, Y. Terauchi, and K. Nagamura, Dynamic Behavior of Planetary Gear (7th Report), Bulletin of the JSME, 22 (1979), 1142-1149.

[3]. Wu X. and Parker R. G., Modal Properties of Planetary Gears With an Elastic Continuum Ring Gear, Journal of Applied Mechanics, 75 (2008), p. 031014.

[4]. F. Cunliffe, J. D. Smith, and D. B. Welbourn, Dynamic Tooth Loads in Epicyclic Gears, Journal of Engineering for Industry, 95 (1974), 578-584.

[5]. M. Botman, Epicyclic Gear Vibrations, Journal of Engineering for Industry, 96 (1976), 811-815.

[6]. R. August and R. Kasuba, Torsional Vibrations and Dynamic Loads in a Basic Planetary Gear System, Journal of Vibration, Acoustics, Stress, and Reliability in Design, 108 (1986), 348-353.

[7]. A. Kahraman, Natural Modes of Planetary Gear Trains, Journal of Sound and Vibration, 173 (1994), 125-130.

[8]. J. Lin and R. G. Parker, Analytical Characterization of the Unique Properties of Planetary Gear Free Vibration, Journal of Vibration and Acoustics 121 (1999), 316-321.

[9]. J. Lin and R. G. Parker, Sensitivity of Planetary Gear Natural Frequencies and Vibration Modes to Model Parameters, Journal of Sound and Vibration, 228 (1999), 109-128.

[10]. J. Lin and R. G. Parker, Structured Vibration Characteristics of Planetary Gears with Unequally Spaced Planets, Journal of Sound and Vibration, 233 (2000), 921-928.

[11]. R. G. Parker, V. Agashe, and S. M. Vijayakar, Dynamic Response of a Planetary Gear System Using a Finite Element/Contact Mechanics Model, ASME Journal of Mechanical Design, 122 (2000), 305-311.

[12]. J. Lin and R. G. Parker, Natural Frequency Veering in Planetary Gears under Design Parameter Variations, Mechanics of Structures and Machines, 29 (2001), 411-429.

[13]. D. R. Kiracofe and R. G. Parker, Structured Vibration Modes of General Compound Planetary Gear Systems, Journal of Vibration and Acoustics, 129 (2007), 1-16

[14]. V. K. Ambarisha and R. G. Parker, Suppression of Planet Mode Response in Planetary Gear Dynamics through Mesh Phasing, ASME Journal of Vibration and Acoustics, 128 (2006), 133-142.

[15]. V. K. Ambarisha and R. G. Parker, Nonlinear Dynamics of Planetary Gears Using Analytical and Finite Element Models, Journal of Sound and Vibration 302 (2007), 577-595.

Copyright © 2009 by ASME

[16]. J. G. Bollinger and R. J. Harker, Instability Potential of High Speed Gearing, Journal of the Industrial Mathematics, 17 (1967), 39-55.

[17]. M. Amabili and A. Rivola, Dynamic Analysis of Spur Gear Pairs: Steady-State Response and Stability of the Sdof Model with Time-Varying Meshing Damping, Mechanical Systems and Signal Processing, 11 (1997), 375-390.

[18]. M. Benton and A. Seireg, Factors Influencing Instability and Resonances in Geared Systems, ASME Journal of Mechanical Design, 103 (1981), 372-378

[19]. C. Nataraj and A. M. Whitman 1997 American Society for Mechanical Engineers Design Engineering Technical Conferences. Paper No. DETC97/¡IB-4018, September, Sacramento, CA. Parameter Excitation Effects in Gear Dynamics.

[20]. G. V. Tordion and R. Gauvin, Dynamic Stability of a Two-Stage Gear Train under the Influence of Variable Meshing Stiffnesses, Journal of Engineering for Industry, 99 (1977), 785-791.

[21]. M. Benton and A. Seireg, Normal Mode Uncoupling of Systems with Time Varying Stiffness, ASME Journal of Mechanical Design, 102 (1980), 379-383

[22]. J. Lin and R. G. Parker, Mesh Stiffness Variation Instabilities in Two-Stage Gear Systems, ASME Journal of Vibration and Acoustics, 124 (2002), 68-76.

[23]. G. Liu and R. G. Parker, Nonlinear Dynamics of Idler Gear Systems, Nonlinear Dynamics, 53 (2008), 345-367.

[24]. P. Velex and L. Flamand, Dynamic Response of Planetary Trains to Mesh Parametric Excitations, Journal of Mechanical Design, 118 (1996), 7-14.

[25]. J. Lin and R. G. Parker, Parametric Instability of Planetary Gears under Mesh Stiffness Variation, Journal of Sound and Vibration, 249 (2002).

[26]. C.-J. Bahk and R. G. Parker, Nonlinear Dynamics of Equally Spaced Planetary Gears, Journal of Computational and Nonlinear Dynamics, submitted (2008).

[27]. R. G. Parker and J. Lin, Mesh Phasing Relationships in Planetary and Epicyclic Gears, Journal of Mechanical Design, 126 (2003), 365-370.

[28]. R. G. Parker, A Physical Explanation for the Effectiveness of Planet Phasing to Suppress Planetary Gear Vibration, Journal of Sound and Vibration, 236 (2000), 561-573.

APPENDIX: EXTENDED OPERATORS

The operators $M$and $K(t)$ in (10) are defined as

$$M\mathbf{a} = \begin{bmatrix} \frac{1}{2\pi}(v - \frac{\partial^2 v}{\partial\theta^2}) \\ \mathbf{Mq} \end{bmatrix},$$

$$K(t)\mathbf{a} = \begin{bmatrix} (k_{bend}L_1 + k_{rus} - k_{rbs}\frac{\partial^2}{\partial\theta^2})v + k_{rn}(t)L_2 v + k_{rn}(t)L_3\mathbf{q} \\ k_{rn}(t)L_4 v + \mathbf{K}(t)\mathbf{q} \end{bmatrix}$$

$$L_1 = -(\frac{\partial^6}{\partial\theta^6} + 2\frac{\partial^4}{\partial\theta^4} + \frac{\partial^2}{\partial\theta^2}),$$

$$L_2 = -\sum_{n=1}^{N}[(\sin^2\alpha_r\frac{\partial^2}{\partial\theta^2} - \cos^2\alpha_r)\delta(\theta-\psi_n) + (\sin\alpha_r\frac{\partial}{\partial\theta} + \cos\alpha_r)\sin\alpha_r\frac{\partial\delta(\theta-\psi_n)}{\partial\theta}]$$

$$L_3\mathbf{q} = \sum_{n=1}^{N}\left[\cos\alpha_r\delta(\theta-\psi_n) - \sin\alpha_r\frac{\partial\delta(\theta-\psi_n)}{\partial\theta}\right]\delta_n$$

$$L_4 v = \begin{bmatrix} \mathbf{b}_r\sum_{n=1}^{N}(\frac{\partial v}{\partial\theta}\sin\alpha_r + v\cos\alpha_r)\Big|_{\theta=\psi_n} \\ \mathbf{0} \\ \mathbf{0} \\ \mathbf{b}_p(\frac{\partial v}{\partial\theta}\sin\alpha_r + v\cos\alpha_r)\Big|_{\theta=\psi_1} \\ \vdots \\ \mathbf{b}_p(\frac{\partial v}{\partial\theta}\sin\alpha_r + v\cos\alpha_r)\Big|_{\theta=\psi_N} \end{bmatrix}$$

$$\mathbf{b}_p = (\sin\alpha_r,\ -\cos\alpha_r,\ -1)^T, \quad \mathbf{b}_r = (-\sin\psi_{rn},\ \cos\psi_{rn},\ 1)^T$$

$$\delta_n = -x_r\sin\psi_{rn} + y_r\cos\psi_{rn} + u_r + \xi_n\sin\alpha_r - \eta_n\cos\alpha_r - u_n$$

$$\mathbf{M} = diag(\mathbf{M}_r, \mathbf{M}_c, \mathbf{M}_s, \mathbf{M}_1, \cdots, \mathbf{M}_N)$$

$$\mathbf{M}_j = diag(m_j, m_j, I_j/r_j^2), \quad j = c, s, 1, \cdots, N, \qquad \mathbf{M}_r = diag[1,\, 1,\, 1/\cos^2\alpha_r]$$

$$\mathbf{K}(t) = \begin{bmatrix} \sum\mathbf{K}_{r1}^n + \mathbf{K}_{rb} & & & \mathbf{K}_{r2}^1 & \cdots & \mathbf{K}_{r2}^N \\ & \sum\mathbf{K}_{c1}^n + \mathbf{K}_{cb} & & \mathbf{K}_{c2}^1 & \cdots & \mathbf{K}_{c2}^N \\ & & \sum\mathbf{K}_{s1}^n + \mathbf{K}_{sb} & \mathbf{K}_{s2}^1 & \cdots & \mathbf{K}_{s2}^N \\ & & & \mathbf{K}_{pp}^1 & & \\ & \text{symmetric} & & & \ddots & \\ & & & & & \mathbf{K}_{pp}^N \end{bmatrix}$$

Copyright © 2009 by ASME

$$\mathbf{K}_{jb} = diag(k_{jx}, k_{jy}, k_{ju}), \quad j = c, s,$$
$$\mathbf{K}_{rb} = \pi diag(k_{rbs} + k_{rus}, k_{rbs} + k_{rus}, 2k_{rus}/\cos^2\alpha_r)$$

k_{rbs} and k_{rus} are uniform radial and tangential distributed stiffnesses, respectively. k^*_{ju} is torsional stiffness with units $F - L/rad$ and $k_{ju} = k^*_{ju}/r_j^2$ with units F/L.

$$\mathbf{K}^n_{pp} = \mathbf{K}^n_{r3} + \mathbf{K}^n_{c3} + \mathbf{K}^n_{s3}$$

$$\mathbf{K}^n_{r1} = k_{rn}(t)\begin{bmatrix} \sin^2\psi_{rn} & -\cos\psi_{rn}\sin\psi_{rn} & -\sin\psi_{rn} \\ & \cos^2\psi_{rn} & \cos\psi_{rn} \\ \text{symmetric} & & 1 \end{bmatrix}$$

$$\mathbf{K}^n_{r2} = k_{rn}(t)\begin{bmatrix} -\sin\psi_{rn}\sin\alpha_r & \sin\psi_{rn}\cos\alpha_r & \sin\psi_{rn} \\ \cos\psi_{rn}\sin\alpha_r & -\cos\psi_{rn}\cos\alpha_r & -\cos\psi_{rn} \\ \sin\alpha_r & -\cos\alpha_r & -1 \end{bmatrix}$$

$$\mathbf{K}^n_{r3} = k_{rn}(t)\begin{bmatrix} \sin^2\alpha_r & -\cos\alpha_r\sin\alpha_r & -\sin\alpha_r \\ & \cos^2\alpha_r & \cos\alpha_r \\ \text{symmetric} & & 1 \end{bmatrix}$$

$$\mathbf{K}^n_{c1} = k_{pn}\begin{bmatrix} 1 & 0 & -\sin\psi_n \\ & 1 & \cos\psi_n \\ \text{symmetric} & & 1 \end{bmatrix},$$
$$\mathbf{K}^n_{c2} = k_{pn}\begin{bmatrix} -\cos\psi_n & \sin\psi_n & 0 \\ -\sin\psi_n & -\cos\psi_n & 0 \\ 0 & -1 & 0 \end{bmatrix}$$

$$\mathbf{K}_{c3} = diag(k_{pn}, k_{pn}, 0)$$

$$\mathbf{K}^n_{s1} = k_{sn}(t)\begin{bmatrix} \sin^2\psi_{sn} & -\cos\psi_{sn}\sin\psi_{sn} & -\sin\psi_{sn} \\ & \cos^2\psi_{sn} & \cos\psi_{sn} \\ \text{symmetric} & & 1 \end{bmatrix}$$

$$\mathbf{K}^n_{s2} = k_{sn}(t)\begin{bmatrix} \sin\psi_{sn}\sin\alpha_s & \sin\psi_{sn}\cos\alpha_s & -\sin\psi_{sn} \\ -\cos\psi_{sn}\sin\alpha_s & -\cos\psi_{sn}\cos\alpha_s & \cos\psi_{sn} \\ -\sin\alpha_s & -\cos\alpha_s & 1 \end{bmatrix}$$

$$\mathbf{K}^n_{s3} = k_{sn}(t)\begin{bmatrix} \sin^2\alpha_s & \cos\alpha_s\sin\alpha_s & -\sin\alpha_s \\ & \cos^2\alpha_s & -\cos\alpha_s \\ \text{symmetric} & & 1 \end{bmatrix}$$

$$\psi_{sn} = \psi_n - \alpha_s, \quad \psi_{rn} = \psi_n + \alpha_r$$

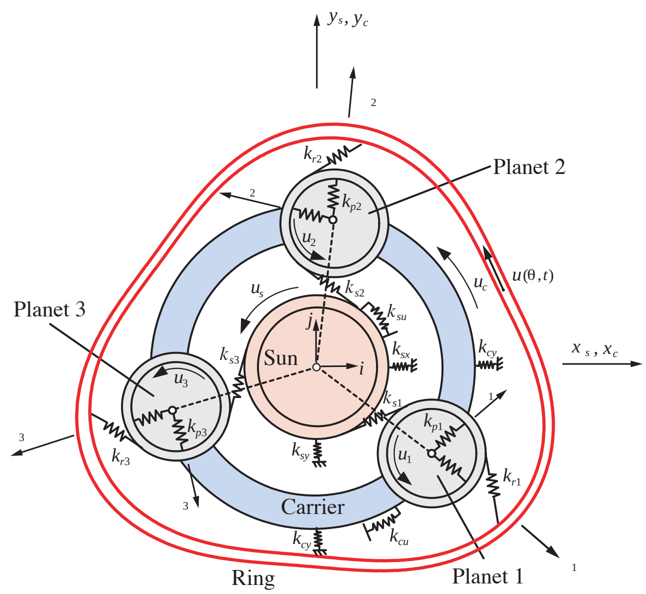

Figure 1. Elastic-discrete model of a planetary gear and corresponding system coordinates. The distributed springs around the ring circumference are not shown.

Copyright © 2009 by ASME

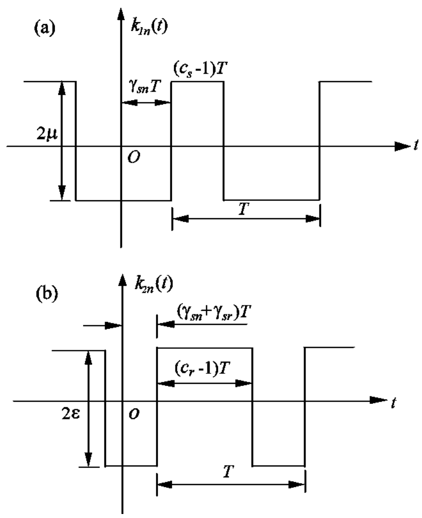

Figure 2. Mesh stiffness variations for the n^{th} (a) sun-planet and (b) ring-planet meshes. c_s, c_r are contact ratios, and γ_{rn} and γ_{sn} are mesh phases.

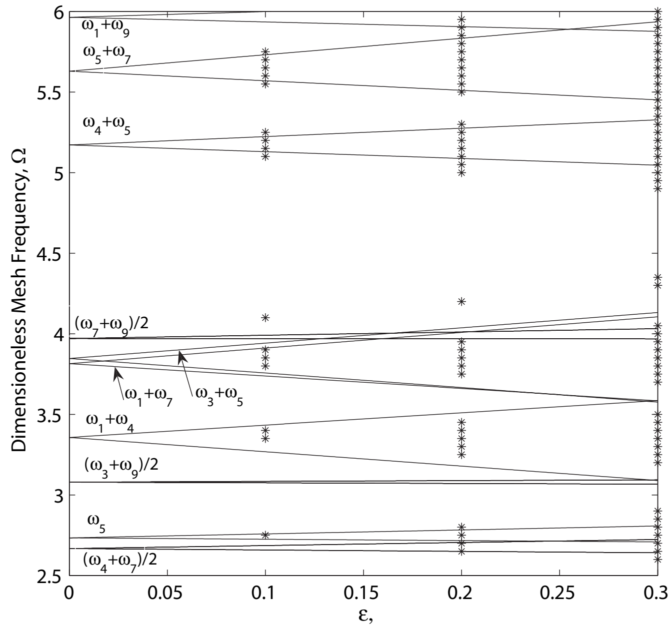

Figure 4. Instability regions for a planetary gear with sequentially phased meshes as $\gamma_{sn} = \left[0, \frac{1}{4}, \frac{1}{2}, \frac{3}{4}\right]$, $\gamma_{sr} = \frac{1}{2}$, $c_s = 1.4$, $c_r = 1.6$, $\varepsilon = \mu$, and other parameters in Table 1. ___ analytical solution; *, numerical solution.**

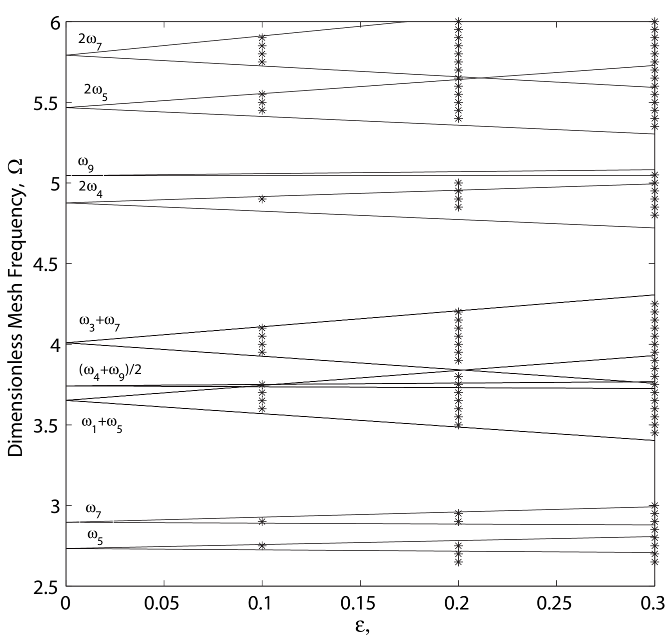

Figure 3. Instability regions for a planetary gear with in-phase meshes as $\gamma_{sn} = 0$, $\gamma_{sr} = \frac{1}{2}$, $c_s = 1.4$, $c_r = 1.6$, $\varepsilon = \mu$, and other parameters in Table 1. ___, analytical solution; *, numerical solution.**

Table 1. Dimensional parameters and dimensionless natural frequencies of an example planetary gear with four equally spaced planets. The designations T, R, P and PR denote translational, rotational, planet and purely ring modes.

Inertias (kg)	$I_r/r_r^2 = 7.6810$, $I_c/r_c^2 = 6$, $I_s/r_s^2 = 2.5$, $I_p/r_p^2 = 2$
Masses (kg)	$m_r = 6.35$, $m_c = 5.43$, $m_s = 0.4$, $m_p = 4$
Stiffnesses (N/m)	$k_{sp} = k_{rp} = 10^8$, $k_{bend} = 5 \times 10^7$, $k_p = k_c = k_s = k_{su} = 5 \times 10^{11}$, $k_{cu} = 5 \times 10^{11}$, $k_{rbs} = 0$, $k_{rus} = 0$
Pressure angle (deg)	$\alpha_s = \alpha_r = 24.6$
Dimensionless natural frequencies	$\omega_1 = \omega_2 = 0.9184$(T), $\omega_3 = 1.113$(R), $\omega_4 = 2.438$(P), $\omega_5 = \omega_6 = 2.733$(T), $\omega_7 = 2.896$(R), $\omega_8 = 4.756$(PR), $\omega_9 = 5.045$(P)

Copyright © 2009 by ASME